Scientia Iranica D (2018) 25(6), 3559–3568

Sharif University of Technology
Scientia Iranica
Transactions D: Computer Science & Engineering and Electrical Engineering
http://scientiairanica.sharif.edu

Estimation of power system Thévenin equivalent based on phasor measurements

B. Alinezhad Osbouei* **and H. Kazemi Karegar**

Faculty of Electrical and Computer Engineering, Shahid Beheshti University (SBU), Tehran, Iran.

Received 8 December 2015; received in revised form 9 November 2016; accepted 5 December 2016

KEYWORDS
Thévenin equivalent;
Phasor Measurement Units (PMU);
Triangulation method;
Phase drift;
Slip frequency.

Abstract. This paper presents a novel algorithm based on phasor measurements for online estimation of power system Thévenin Equivalent (TE) from a generator terminal. Three consecutive phasor measurements of generator terminal voltage and current are used to estimate the system TE. In a real network, deviation of system frequency from its nominal value produces some phase drifts in consecutive phasors reported by Phasor Measurements Units (PMUs). To correct the phase drift and synchronize the reported phasors with the same reference, an improved triangulation method is developed. The improved method uses a virtual vector in its structure. This vector alleviates negative impacts of improper data resulting from noise or disturbances, which make the simple triangulation method useless. The algorithm is tested on standard NE-39 network and is implemented in Shahid Beheshti University's (SBU) protection laboratory to verify the results in practice. The obtained results show that the new method can efficiently estimate the Z_{th} in online mode under steady-state and transient conditions.

1. Introduction

Wide Area Measurement Systems (WAMS) have been developed for better operation and modelling of power system [1], monitoring [2], and state estimation [3]. In WAMS, all measurements are synchronized with the same reference by means of Phasor Measurement Units (PMUs), which are installed at some power system terminals. When synchronized phasor values are available, online estimation of system parameters, such as Thévenin Equivalent (TE), can be done more conveniently and accurately.

System TE can be used in various fields of studies. Generally, in a power system, TE is estimated from a load or generator terminal. The main importance of TE from a load terminal is apparent in Voltage Stability Assessment (VSA) studies. In [4-5], the voltage stability was evaluated by analyzing the ratio of Thévenin impedance (Z_{th}) to the load impedance (Z_L). In [6-7], the voltage stability of power system, including large wind generations, were examined with TE estimation and capacity chart of wind turbines.

For a generator terminal, which is the focus of this paper, system TE is usually used for fault location problems and stability studies. In [8], TE and some curve fitting techniques were used to estimate the exact location of a fault on a HV transmission line. Online estimation of TE from a generator terminal in a power network can be used for estimating its transient stability in the case of fault by reducing the connected network to a Single Machine Infinite Bus (SMIB) system and using Equal Area Criterion (EAC) to determine the generator stability. Furthermore, for permanent dynamic interactions and frequency oscillations between the generator and power system, it is highly difficult to calculate the TE in this case. This

*. *Corresponding author.*
E-mail addresses: b_alinejad@sbu.ac.ir (B. Alinezhad Osbouei); h_kazemi@sbu.ac.ir (H. Kazemi Karegar).

doi: 10.24200/sci.2017.4373

requires faster and more stable algorithms with some features as resistance against noise, light computations, and phase drift correction.

Recent studies have shown that synchronized measurements can facilitate on-line estimation of TE. In [9], TE was calculated by generator voltage and current phasors for designing an adaptive voltage regulator. In [10], an initial estimation of TE from a load terminal was established. It then converged to exact value using an incrementally based algorithm depending on the load impedance variations recorded by PMUs. In [11], the Tellegen theorem was applied to two consecutive phasor measurements to estimate the Z_{th}. In [12], the Z_{th} was estimated from an improved recursive method, using differential variables to reflect parameters changes. A mathematical equation was proposed in [13] to correct the phase drift caused by the slip frequency between PMU successive phasors. Then, the corrected phasors were used for TE estimation from a generator terminal. In [14], three consecutive phasor measurements of generator voltage and current were used to correct the phase drift and TE estimation. In [15-16], a recursive least square estimation technique was used to estimate the online Z_{th} for tracking the voltage stability from a load terminal. In [17], authors proposed a new method based on the rate of the change of frequency obtained from PMU measurement in order to correct the phase drift and calculate the TE. In addition, Abdelkader and Morrow [18] developed a new method for TE estimation in the case of a change in system parameter and measurement errors.

In this paper, a new method based on analyses of generator voltage and current phasors is proposed to estimate the online TE from the generator terminal. By using three successive pairs of generator current and voltage phasors, two phasor triangles are constructed based on a virtual vector explained in the next chapter. Each triangle is intended to correct the phase drift of each measurement and an initial estimation of the Z_{th} will be obtained. Finally, a method to adopt the best estimation is formulated.

The algorithm is verified by simulations in steady-state and transient conditions on the 39-Bus ($NE-39$) network. Moreover, the proposed method is implemented in university's protection laboratory. Also, PMU module is coded in MATLAB software based on IEEE C37.118 standard to calculate the generator voltage and current phasors both in simulations and laboratory tests. The obtained practical and simulation results show that the new online estimation method has a suitable capability and accuracy in transient conditions.

In the second Section, the proposed algorithm is described. Simulations and practical results are shown in Sections 3 and 4, respectively.

2. Problem statement and proposed algorithm

Suppose that a generator is connected to a power system as shown in Figure 1. The TE seen from generator terminal ($B1$) reduces the connected power system shown with the dashed line to equivalent impedance and a voltage source, as shown in Figure 2.

If connected power system is large enough compared with generator $G1$ and the measurements periods are short enough, then one can assume that the V_{th} remains constant during two consecutive measurements. Accordingly, TE can be calculated by two consecutive current and voltage phasors (V_{G1}, I_{G1}) and (V_{G2}, I_{G2}), recorded at generator terminal as follows:

$$Z_{th} = \frac{V_{G1} - V_{G0}}{I_{G1} - I_{G0}}, \tag{1}$$

$$V_{th} = V_{G1} - Z_{th} I_{G1}. \tag{2}$$

In Eqs. (1) and (2), 0 and 1 subscripts denote the first and second measurements, respectively. However, this method is simple, yet cannot be used in a real network. In real networks, there is always some frequency deviation from its nominal value. This deviation, however very small, produces unwanted phase drift between consecutive measurements. Therefore, two phasors will not be synchronized on the same reference, and when used in Eqs. (1) and (2) without correction, ambiguous and noisy results are inevitable.

Figures 3 and 4 show a real image of frequency and the phase angle of voltage phasor transmitted from

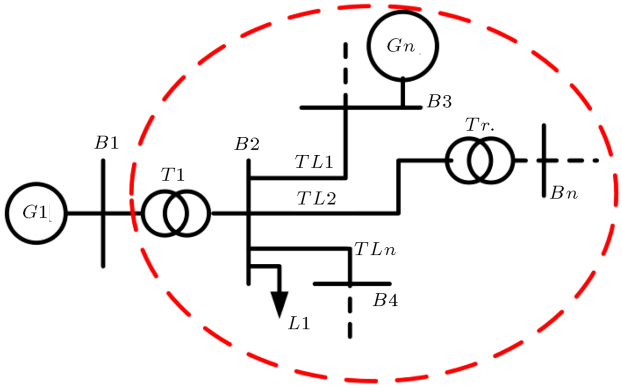

Figure 1. Typical power system.

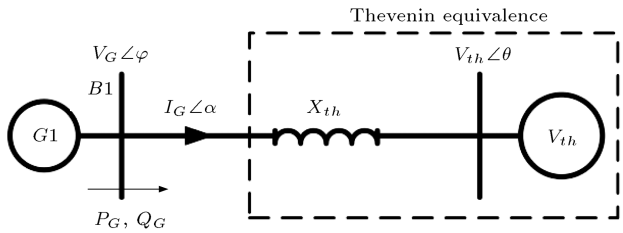

Figure 2. TE from generator terminal ($B1$).

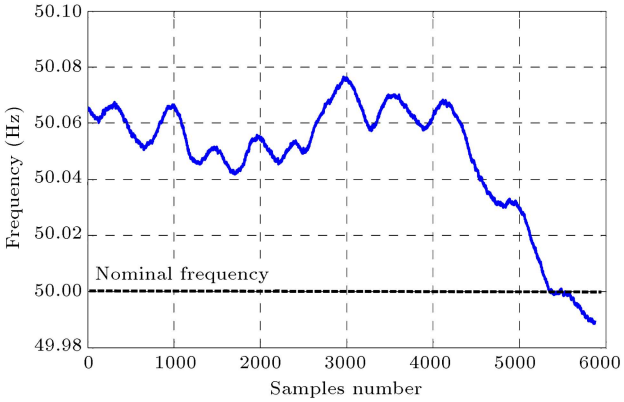

Figure 3. Actual frequency of a 400 kV substation reported by PMU at PDC.

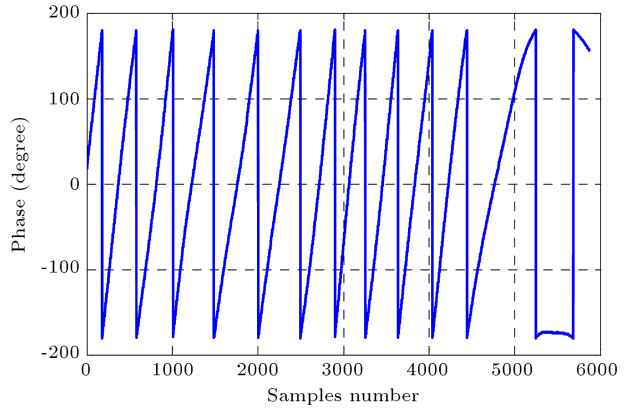

Figure 4. The phase angle of reported voltage phasor at PDC.

a PMU installed at a 400 kV substation in Iran power grid. Data are obtained from Phasor Data Concentrator (PDC) center developed in Iran Grid Management Company (IGMC). As depicted in Figure 3, at the time of phasor calculations, the frequency of the system was almost higher than the nominal frequency (50 Hz). As PMU reporting rate is normally constant (20 ms for respected PMU), in PDC center, the phase angle of any recorded phasor is not constant and changes from $-180°$to $180°$ permanently, as shown in Figure 4. This is called "phase drift", meaning that two consecutive phasors are not synchronized on the same reference. Figure 5 shows the relevant Z_{th} value calculated directly by Eq. (1) from the mentioned data. As is clear, the calculated impedance contains considerable fluctuations from its exact value. Therefore, a method is required to correct the phase drift and synchronize the consecutive phasors on the same reference.

A basic triangulation method to correct the phase drift with three consecutive measurements is proposed in [14], briefly discussed in the Appendix. Consider three measurement pairs at generator terminal available as (V_1, I_1), (V_2, I_2), and (V_3, I_3). The 1, 2, and 3 subscripts denote the first, second, and third

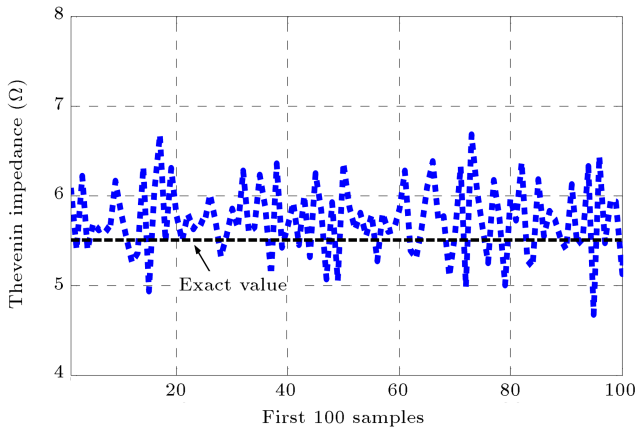

Figure 5. TE for a 400 kV substation using Eq. (1) and data obtained from PDC.

measurements, respectively. If the phase angle of the first measurement is taken as a reference, the phase of the second and third measurements can be synchronized with first one as ($V_2e^{-j\alpha 1}$, $I_2e^{-j\alpha 1}$) and ($V_3e^{-j\alpha 2}$, $I_3e^{-j\alpha 2}$), respectively. The main problem is finding the value of (α_1, α_2). According to [14], if three consecutive phasors belong to a unique Z_{th}, then the determinant of Eq. (A.1) should be zero and lead to a phasor triangle construction by A, B, and C vectors. (See Eqs. (A.2), (A.3), and Figure (A.1) of the Appendix). Using this triangular structure, (α_1, α_2) can be found and consecutive phasors could be synchronized with the same reference; thus, phase drift is corrected.

This method is very useful; however, the accuracy of the results depends on the measurement samples [19]. Experience suggests that, in many cases, the values of (α_1, α_2) are complex which cannot be accepted. The main reason is based on the fact that when system is in normal operation, independent of the amount of phase drift, the values of vectors A, B, and C are close to zero. This implies that Eq. (A.2) is intentionally zero, and the values of (α_1, α_2) cannot be calculated practically. In addition, even if there is a real answer, two alternative solutions as (α_1', α_2') and (α_1'', α_2'') exist according to Eqs. (A.4) and (A.5). According to [19], the problem of a solution yielding a valid or invalid answer for phase drift correction is unknown and depends on the measured data. Therefore, this method requires some extra assistance to obtain better results. In this paper, a modified triangulation method is proposed to solve the problem as in the following procedures:

Step 1. Suppose that three consecutive measurement pairs as (V_1, I_1), (V_2, I_2), and (V_3, I_3) at generator terminal are available. Assume (V_1, I_1) as reference measurements to synchronize the others. If there is a real (not complex) answer for (α_1, α_2), then go to Step 2, otherwise go to Step 3.

Step 2. In this step, (α_1, α_2) can be obtained from basic triangulation method from Eqs. (A.4) or (A.5). The problem is that two answers for (α_1, α_2) as (α'_1, α'_2) and (α''_1, α'_2) are available in which the correct one should be adopted for phase drift correction. Therefore, the first three Z'_{th}s are calculated from (V_1, I_1) as well as corrected values of (V_2, I_2) and (V_3, I_3) based on (α'_1, α'_2) as follows:

$$Z'_{21} = \frac{V_2 e^{-j\alpha'_1} - V_1}{I_2 e^{-j\alpha'_1} - I_1}, \tag{3}$$

$$Z'_{31} = \frac{V_3 e^{-j\alpha'_2} - V_1}{I_3 e^{-j\alpha'_2} - I_1}, \tag{4}$$

$$\begin{aligned} Z'_{32} &= \frac{V_3 e^{-j\alpha'_2} - V_2 e^{-j\alpha'_1}}{I_3 e^{-j\alpha'_2} - I_2 e^{-j\alpha'_1}} \\ &= \frac{(V_3 e^{-j\alpha'_2} - V_1) - \left(V_2 e^{-j\alpha'_1} - V_1\right)}{\left(I_3 e^{-j\alpha'_2} - I_1\right) - (I_2 e^{-j\alpha'_1} - I_1)} \\ &= \frac{A' Z'_{31} - B' Z'_{21}}{A' - B'}, \end{aligned} \tag{5}$$

$$\begin{aligned} E' = &\Big(\left(|Z'_{21}| - |Z'_{31}|\right)^2 + \left(|Z'_{21}| - |Z'_{32}|\right)^2 \\ &+ \left(|Z'_{31}| - |Z'_{32}|\right)^2 \Big). \end{aligned} \tag{6}$$

In Eq. (5), A' and B' can be obtained from $(I_3 e^{-j\alpha'_2} - I_1)$ and $(I_2 e^{-j\alpha'_1} - I_1)$, respectively. E' is the calculation error when (α_1, α_2) is used. The two cycle time spans of the three consecutive measurements are noticeably short; therefore, in theory, the values of Z'_{21}, Z'_{31}, and Z'_{32} must be identical and E' be zero. However, this will not be put into practice.

Next, other three Z''_{th}s are also calculated from (V_1, I_1) and corrected values of (V_2, I_2) and (V_3, I_3), except (α''_1, α''_2), as follows:

$$Z''_{21} = \frac{V_2 e^{-j\alpha''_1} - V_1}{I_2 e^{-j\alpha''_1} - I_1}, \tag{7}$$

$$Z''_{31} = \frac{V_3 e^{-j\alpha''_2} - V_1}{I_3 e^{-j\alpha''_2} - I_1}, \tag{8}$$

$$\begin{aligned} Z'_{32} &= \frac{V_3 e^{-j\alpha''_2} - V_2 e^{-j\alpha''_1}}{I_3 e^{-j\alpha''_2} - I_2 e^{-j\alpha''_1}} \\ &= \frac{(V_3 e^{-j\alpha''_2} - V_1) - \left(V_2 e^{-j\alpha''_1} - V_1\right)}{\left(I_3 e^{-j\alpha''_2} - I_1\right) - (I_2 e^{-j\alpha''_1} - I_1)} \\ &= \frac{A'' Z''_{31} - B'' Z''_{21}}{A'' - B''}, \end{aligned} \tag{9}$$

$$\begin{aligned} E'' = &\Big(\left(|Z''_{21}| - |Z''_{31}|\right)^2 + \left(|Z''_{21}| - |Z''_{32}|\right)^2 \\ &+ \left(|Z''_{31}| - |Z''_{32}|\right)^2 \Big). \end{aligned} \tag{10}$$

In Eq. (9), A'' and B'' can be obtained from $(I_3 e^{-j\alpha''_2} - I_1)$ and $(I_2 e^{-j\alpha''_1} - I_1)$, respectively, and E'' is calculation error. The values of E' and E'' are used for the adopting criteria. To choose the correct answer for (α_1, α_2), the following criterion is used:

$$(\alpha_1, \alpha_2) = \begin{cases} (\alpha'_1, \alpha'_2) \text{ if } & E' \le E'' \\ (\alpha''_1, \alpha''_2) \text{ if } & E' > E'' \end{cases} \tag{11}$$

According to Eq. (11), the correct choice between (α'_1, α'_2) and (α''_1, α''_2) is the one that produces less error, based on which phase drift correction and TE are calculated.

Step 3. There is not a real solution for (α_1, α_2), and complex values may be adopted which cannot be accepted and TE calculation is not possible. To overcome this, the effect of phase drift on each vector will be studied separately. The proposed correction algorithm is as below:

Step 3.1. Assume vector A as the reference vector, and assume that the slip frequency affects only vector B and does not have effect on C. Both size and angle of vector B will be changed to form a triangle with the other two vectors. Therefore, a virtual vector called B^*, which is equal to $B^* = -A - C$, is produced for estimating the phase drift of vector B. This is shown in Figure 6. As C is assumed unaffected, according to Eq. (A.3), the equivalent phase drift of B can only be related to the third measurement pairs. This value (β_0) and related Thévenin impedance (Z^{B*}_{th}) can be calculated as follows:

$$\begin{aligned} \beta_0 &= \alpha_B - \theta_B \\ &= \text{angle}\,(B^*) - \text{angle}\,(B) \\ &= \text{angle}\,(-A - C) - \text{angle}\,(B), \end{aligned} \tag{12}$$

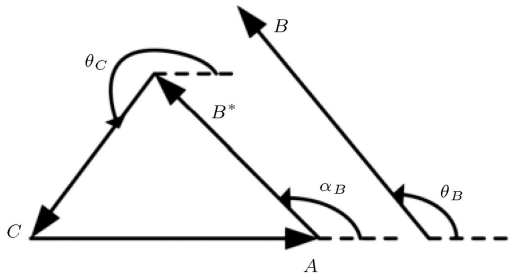

Figure 6. Construction of B^* vector.

$$Z_{th}^{B*} = \left(\frac{\bar{V}_1 - \bar{V}_3^C}{\bar{I}_1 - \bar{I}_3^C}\right)$$

$$= \left(\frac{\overline{V_1} - \overline{V_3}\exp(-j\beta_0)}{\overline{I_1} - \overline{I_3}\exp(-j\beta_0)}\right). \quad (13)$$

Step 3.2. Independent of Step 3-1 and based on Figure 7, it is assumed that vector B is not affected and virtual vector C^* is constructed to form a triangle with the other two ones. The equivalent phase drift of vector C is equal to β_1 and can be obtained as:

$$\beta_1 = \alpha_C - \theta_C = \text{angle}(C^*) - \text{angle}(C)$$

$$= \text{angle}(-B - A) - \text{angle}(C). \quad (14)$$

The corresponding value of the $Z_{th}^{(C*)}$ is obtained from the first and second measurement pairs. In this step, the calculated phase drift is related to the second measurement pairs.

$$Z_{th}^{B*} = \left(\frac{\bar{V}_1 - \bar{V}_2^C}{\bar{I}_1 - \bar{I}_2^C}\right)$$

$$= \left(\frac{\overline{V_1} - \overline{V_2}\exp(-j\beta_1)}{\overline{I_1} - \overline{I_2}\exp(-j\beta_1)}\right). \quad (15)$$

Step 3-3. For the final estimation of Z_{th}^{Final}, Eq. (5) is rewritten as follows:

$$Z_{th}^{\text{Final}} = \frac{AZ_{th}^{B*} - BZ_{th}^{C*}}{A - B}, \quad (16)$$

where $A = (I_3 e^{-j\beta} - I_1)$ and $B = (I_2 e^{-j\beta 1} - I_1)$. The value of the V_{th} could be calculated from the Z_{th}^{Final} and any corrected phasors as follows:

$$V_{th} = \bar{V}_1 - Z_{th}^{\text{Final}}\bar{I}_1 = \bar{V}_2^C - Z_{th}^{\text{Final}}\bar{I}_2^C$$

$$= \bar{V}_3^C - Z_{th}^{\text{Final}}\bar{I}_3^C. \quad (17)$$

Since $A = V_1 I_2 - V_2 I_1$, in all steps, it has a constant amount of drift. This is a general case which allows the algorithm to adopt any of the vectors as the reference. This will not affect the result of calculations.

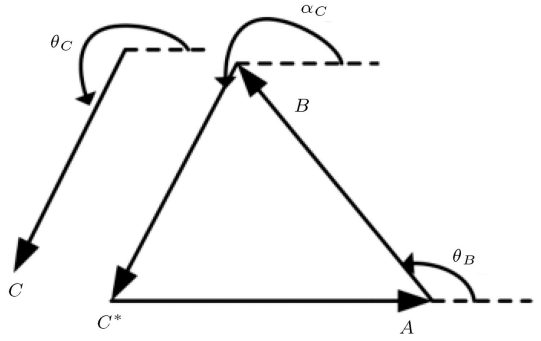

Figure 7. Construction of C^* vector.

3. Simulations and results

Standard 39-Bus ($NE-39$) test system shown in Figure 8 is simulated in time domain in Power-factory® DigSilent software and is used to verify the proposed method. The percent loading of branches is obtained from power flow result. All necessary voltages and currents are sampled with a frequency of 2 kHz by the software. These data are then transferred to MATLAB program for calculating voltage and current phasors with a PMU coded based on IEEE C37.118 standard. The ability of the proposed method is tested in two scenarios: load disturbance and line faults. The objective is to calculate TE seen from the generator $G2$ terminal, which is terminal no. 32. Before any disturbance, all generators are in normal operation conditions and operational frequency of the network is constant. The phase drift values before disturbances are negligible.

3.1. Load disturbance

A load of 129 MW and 36 MVAR at terminal no. 26 is switched on in 10 seconds. Before this time, the system was simulated until it reached a steady-state condition, which is a constant voltage and constant frequency for the whole system. The values of the Z_{th} and X_{th} seen from generator $G2$ are shown in Figure 9. The obtained results are also compared with two other methods' results. The first method indicated by "Simple Method" in Figure 9 is obtained directly from Eq. (1) without phase drift correction. In other words, the consecutive phasors obtained from PMU are directly used in Eq. (1) for impedance calculation. Another one indicated by Abdelkader and Morrow's method [14] is calculated from the algorithm developed in [14] where a simple triangulation method is used to correct the phase drift.

As the entered load is far from generator $G2$ and is small compared with the network size, the Z_{th} seen from terminal no. 32 will not change significantly. However, the load switching will cause some small variations in system frequency. These variations produce a phase drift in PMU reporting phasors. In case of phase drift, the voltage and current phasors of terminal no. 32 reported by PMU will rotate in its real-imaginary plane, as shown in Figure 10.

This rotation is valid for a few seconds before and after the load switching. In Figure 10, the reported phasors before the load switching are concentrated at a small circle, meaning that no phase drift exists. Outer points are related to the reported phasors after load switching whose voltage and current phasors rotate on a circle. The magnitude of reported phasors is almost constant; however, a significant phase drift is observed. In this area, a phase drift correction is inevitable for synchronizing the consecutive measurements.

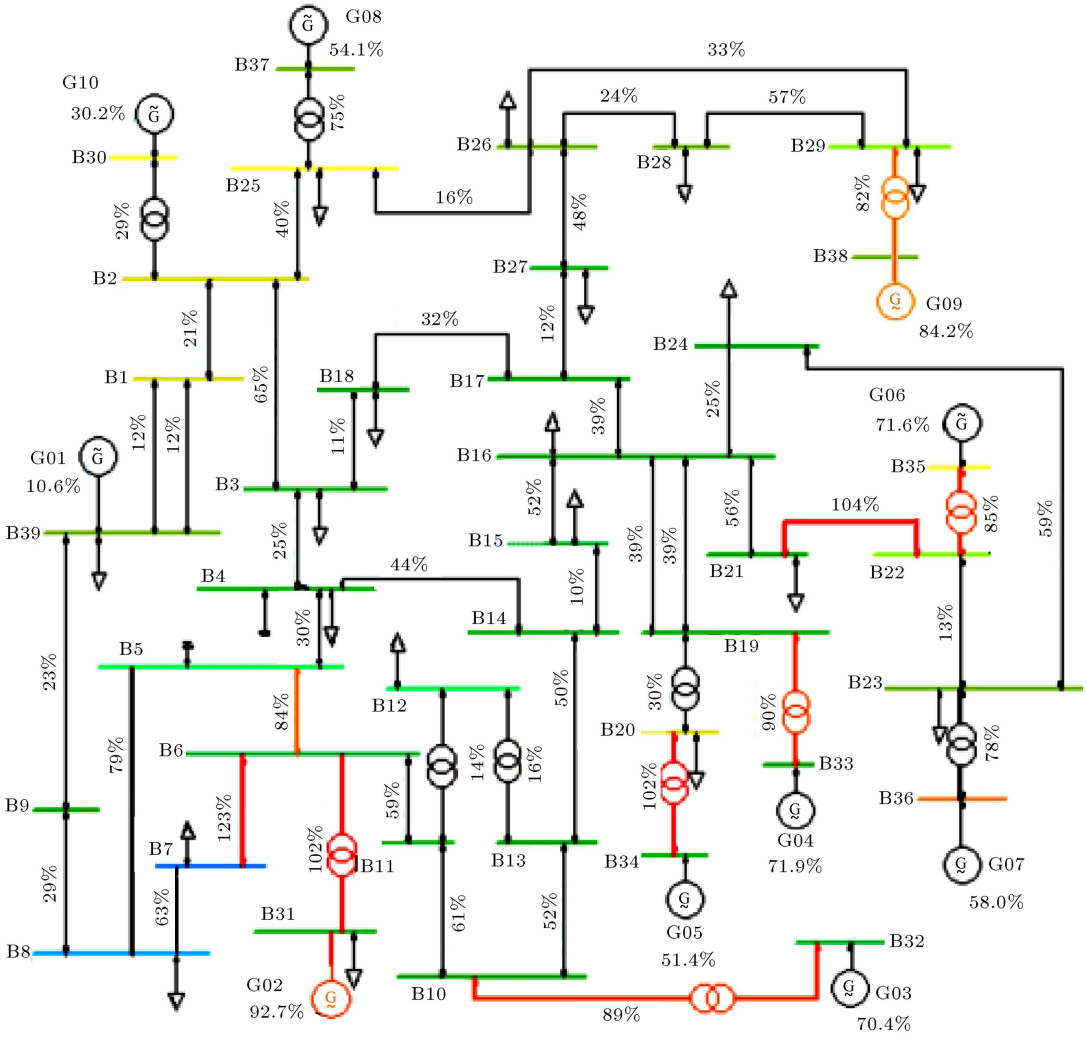

Figure 8. $NE-39$ test system with equipment loading.

As can be seen from Figure 9, the fluctuations of the proposed method are much lower than those of the other two methods, especially in the estimation of X_{th}. The exact values for system Thévenin impedances seen from terminal no. 32 are obtained from Ansi short-circuit calculations in DigSilent software and are 0.53 Ω for Z_{th} and 0.43 Ω for X_{th}, respectively.

3.2. System faults

For testing the proposed method's ability in severe conditions, the network will face single and double three-phase faults near generator $G2$. First, a single three-phase fault is simulated on the line connecting terminals 6 to 7 in 10 seconds. This line is adopted because its loading is higher than the other lines' loading, connecting $G2$ to the rest of the network, and so, more severe conditions will happen.

The obtained X_{th} by the proposed method and two other methods are shown in Figure 11(a). As the fault is near the generator, the X_{th} is reduced significantly. The exact value is 0.167 Ω. Results of all methods are accepted; however, the proposed method's estimation is better, especially at the instance of the fault. The estimation error is about 4.2%.

Furthermore, a double three-phase fault is also simulated. In this case, both lines connecting terminals 6 to 5 and 7 in Figure 8 are short-circuited simultaneously with a three-phase fault. As expected, the value of X_{th} is reduced again, which is shown in Figure 11(b). The exact value in this case is 0.11 Ω. As can be seen in this case, the algorithm response is more accurate than the two other methods, showing fewer fluctuations. The estimation error of the proposed algorithm is lower than 10%.

4. Practical test

The validity of the proposed method is verified in a practical test done in the protection laboratory of SBU University. Figures 12 and 13 show the components and single-line diagram of the test system. A DC motor coupled with a 3-phase synchronous generator

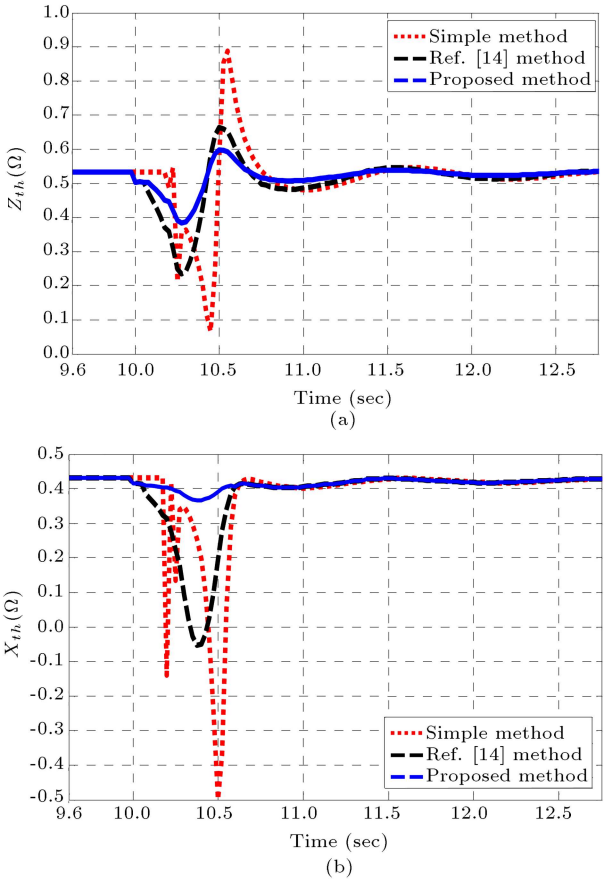

Figure 9. Obtained TE in the case of load disturbance: (a) Value of Z_{th} in Ω, and (b) value of X_{th} in Ω.

is connected to the laboratory network. A digital scope is used to save the generator voltage and current via an appropriate voltage and current transformers. The system and sampling frequency are 50 Hz and 1 kHz, respectively. A synchronizing bracket composed of a synchronizer and a switch is used to parallel the generator to the laboratory network.

After paralleling the generator to the laboratory network, phase voltage and current of generator terminal are saved by means of a digital scope for one second. These data are used to estimate the Thévenin impedance from generator point of view in a steady-state condition. A digital low-pass filter is implemented to extract the first harmonic of voltage and current signals. Voltage and current phasors are calculated by means of a simulated PMU according to IEEE C137.118 standard.

Due to the network voltage inconsistency during the test, some oscillations are observed. The magnitude of the network voltage recorded by the digital scope is shown in Figure 14. Since the generator does not connect to an ideal network, some disturbances at its terminal voltage are expected. However, the proposed algorithm still shows acceptable results. Figure 15 shows the estimated value of the X_{th} obtained from the

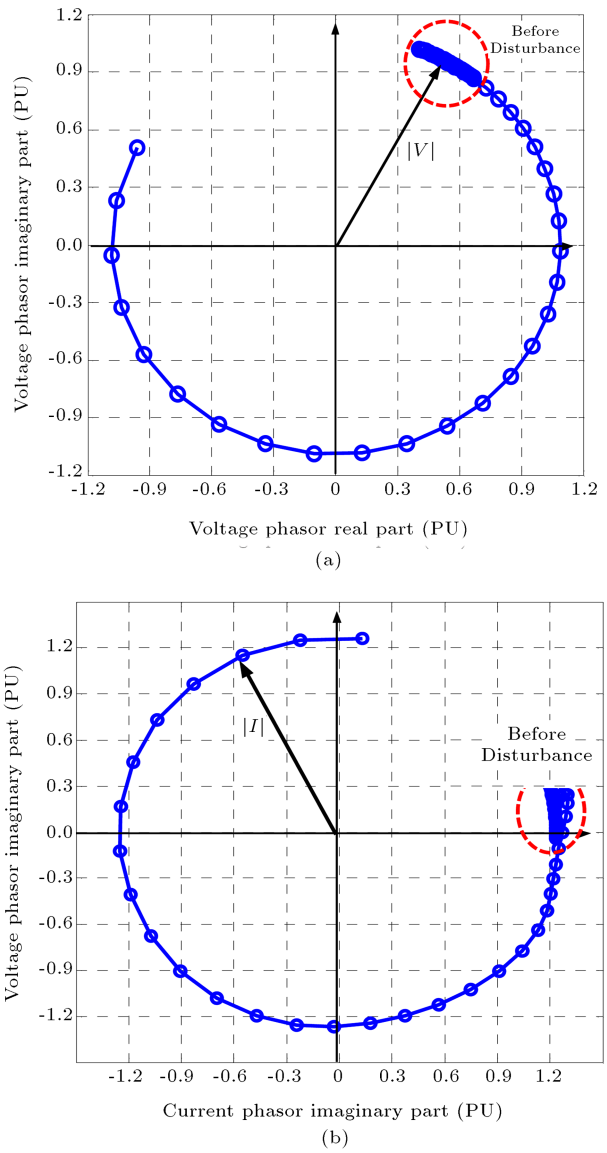

Figure 10. Reported phasors of bus no. 32 for load disturbance: (a) Voltage phasor (PU), and (b) current phasor (PU).

proposed method and two other methods. Abdelkader and Morrow's method [14] does not have an acceptable result between 0.2 s and 0.4 s, probably because it did not calculate the phase drifts correctly at this period. Result of a simple method shown by the dotted line in Figure 15 has significant oscillations in all times and absolutely fails in impedance estimation.

The estimated values for the R_{th} are shown in Figure 16. As previous stated, results of the proposed algorithm are better. Abdelkader and Morrow's method [14] loses its accuracy after 0.6 seconds; approximately after 0.8 seconds, the calculation is not possible due to the resulting complex values for (α_1, α_2). At this section, the proposed algorithm has an answer with good accuracy.

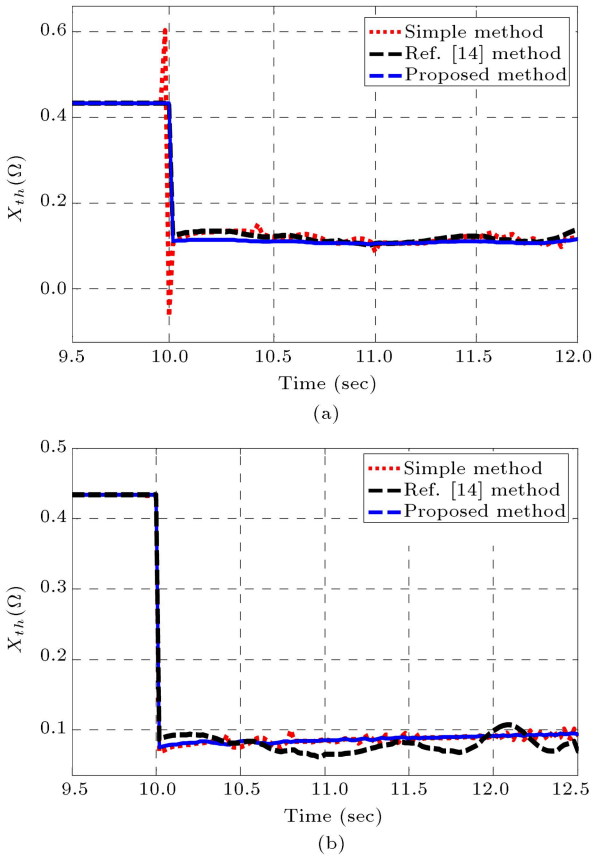

Figure 11. Obtained X_{th} in case of fault and (a) Line single three-phase fault, and (b) line double three-phase fault.

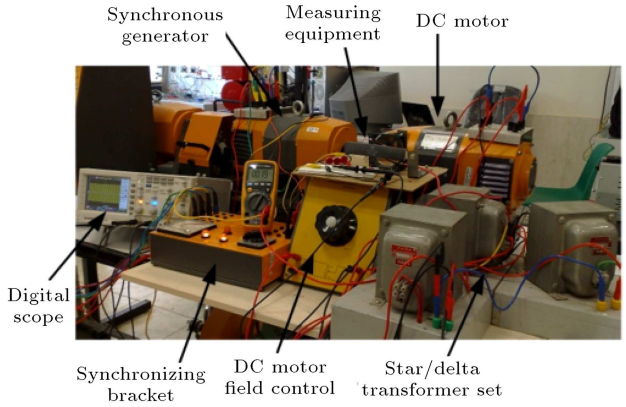

Figure 12. Laboratory test system.

5. Conclusion

A new method for TE estimation based on PMU data was presented. The phase drift problem was corrected via a virtual vector that contributed to the simple triangulation method. The algorithm was tested and verified with a standard IEEE 39-Bus test network in both steady-state and faulty conditions. Load switching and single and common three-phase faults were simulated by DigSilent software in time domain

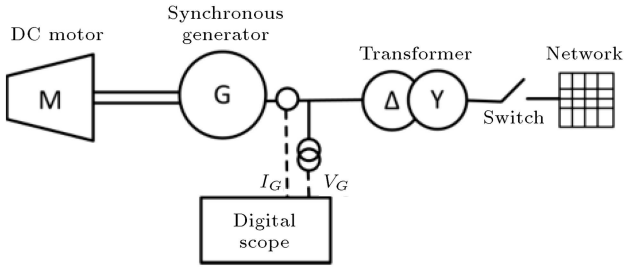

Figure 13. Laboratory test system to calculate network TE.

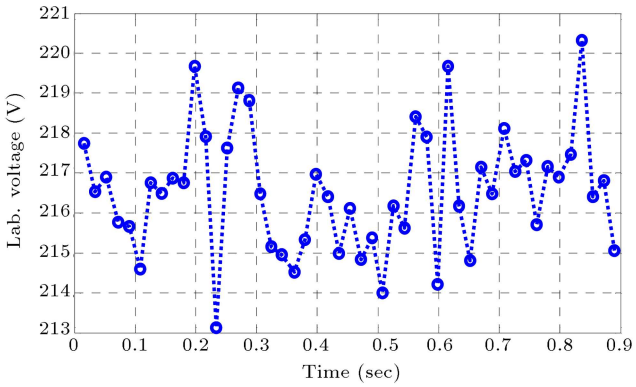

Figure 14. Laboratory network voltage during the test.

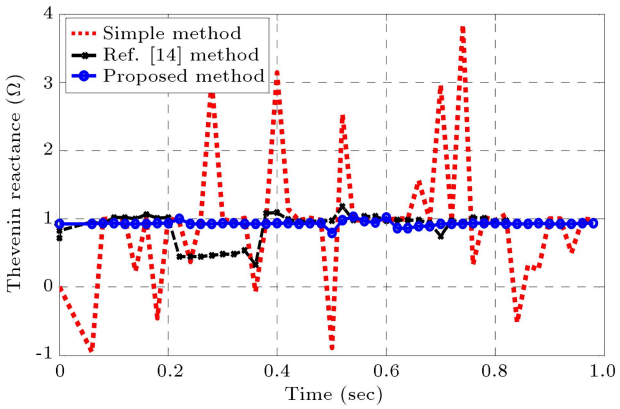

Figure 15. Thévenin reactance (X_{th}) for laboratory test system.

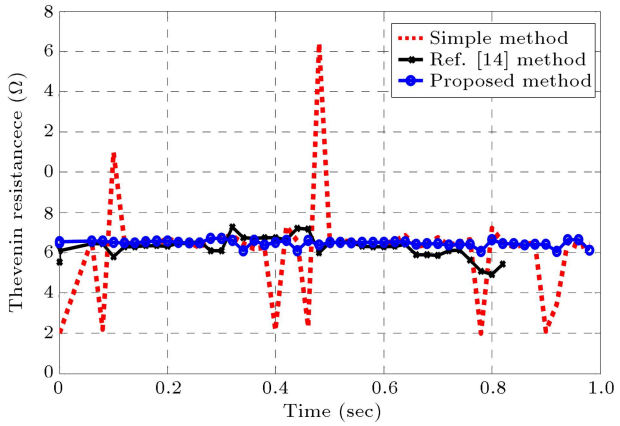

Figure 16. Thévenin resistance (R_{th}) for laboratory test system.

to produce phase drift. PMU was also simulated in MATLAB based on IEEE C37.118 standard. The results of the proposed method were compared with those of simple methods and methods of Abdelkader and Morrow [14]. The obtained results show that the new method has better results in both steady-state and transient conditions. In steady-state condition, the error is less than 1%, and in case of transient condition, it shows very interesting results compared with other methods. Moreover, a practical test system in protection laboratory of SBU University was also implemented, whose obtained results show the accuracy of the proposed method.

Acknowledgement

All services and guidance from Iran Grid Management Company (IGMC) for the preparation and availability of information of the network phasors data are highly appreciated.

References

1. Alinezhad, B., Akbari, M., and Kazemi, H. "PMU-based distribution network load modelling using harmony search algorithm", *17th Conf. on Electrical Power Distribution Networks (EPDC)*, Tehran, Iran, pp. 1-6 (2012).
2. Safdarian, A., Aminifar, F., Fotuhi-Firuzabad, M., and Shahidehpour, M. "A Multi-Objective Framework for Enhancing the Reliability and Minimizing the Cost of PMU Deployment in Power Systems", *Scientia Iranica*, **23**(6), pp. 2917-2927 (2016).
3. Soni, S., Bhil, S., and Mehta, D. "Linear state estimation model using phasor measurement unit (PMU) technology", *9th Int. Conf. on Elect. Engin., Computing Science and Automatic Control (CCE)*, Mexico, pp. 1-6 (2012).
4. Chebbo, A., Irving, M.R., and Sterling, M.J.H. "Voltage collapse proximity indicator, behavior and implications", *IEE Gen. Trans. and Dist.*, **139**(3), pp. 241-252 (1992).
5. Elkateb, M., Abdelkader, M.S., and Kandil, M.S. "Linear indicator for voltage collapse in power systems", *IEE Gen. Trans. and Dist.*, **144**(2), pp. 139-146 (1997).
6. Abdelkader, M.S. and Flynn, D. "Graphical determination of network limits for wind power integration", *IET Gen. Trans. Dist.*, **3**(9), pp. 841-849 (2009).
7. Abdelkader, M.S. and Fox, B. "Voltage stability assessment for system with large wind power generation", *44th Int. Universities Power Engineering Conf.*, Glasgow, United Kingdom, pp. 1-6 (2009).
8. Al-Mohammed, A.H. and Abido, M.A. "A fully adaptive PMU-based fault location algorithm for series-compensated lines", *IEEE Trans. on Power Syst.*, **29**(5), pp. 2129-2137 (2014).
9. Fusco, G. and Russo, M. "Adaptive voltage regulator design for synchronous generator", *IEEE Trans. on Energy Conv.*, **23**(3), pp. 946-956 (2008).
10. Corsi, S. and Taranto, G. "A real time voltage instability identification algorithm based on local phasor measurements", *IEEE Trans. on Power Syst.*, **23**(3), pp. 1271-1279 (2008).
11. Smon, I., Verbic, G., and Gubina, F. "Local voltage stability index using Tellegen's theorem", *IEEE Trans. on Power Syst.*, **21**(3), pp. 1267-1275 (2006).
12. Munan, W., Baozhu, L., and Zhelin, D. "An improved recursive assessment method of Thevenin equivalent parameters based on PMU measurement", *Power Eng. and Auto. Conf. (PEAM)*, Wuhan, China, pp. 372-375 (2011).
13. Abdelkader, M.S. "Online Thevenin's equivalent using local PMU measurements", *Int. Conf. on Renewable Energy and Power Quality (ICREPQ 11)*, Las Palmas, Spain, pp. 1-4 (2010).
14. Abdelkader, M.S. and Morrow, D. "Online tracking of Thévenin equivalent parameters using PMU measurements", *IEEE Trans. on Power Syst.*, **27**(2), pp. 975-983 (2012).
15. Tsai, S. and Wong, K. "On-line estimation of Thevenin equivalent with varying system states", *IEEE Power and Energy Society General Meeting-Conv. and Delivery of Elect. Energy in the 21st Century*, Pittsburgh, USA, pp. 1-7 (2008).
16. Corsi, S. and Taranto, G.N. "Voltage instability alarm by real-time predictive indicators", *IEEE Power and Energy Society General Meeting*, pp. 1-10 (2012)
17. Alinezhad, B. and Karegar, H.K. "On-line Thevenin impedance estimation based on PMU data and phase drift correction", *IEEE Trans. on Smart Grid*, to be published (2016).
18. Abdelkader, S.M. and Morrow, D.J. "Online Thévenin equivalent determination considering system side changes and measurement errors", *IEEE Trans. on Power Syst.*, **30**(5), pp. 2716-2725 (2015)
19. Vanouni, M. "Discussion of "Online Tracking of Thévenin Equivalent Parameters Using PMU Measurements", *IEEE Trans. on Power Syst.*, **28**(2), p. 1899 (2013).

Appendix

Based on the theory developed in [14], the necessary and sufficient condition for the presence of valid TE at a node is provided, when Eq. (A.1) is valid, which is as follows:

$$\begin{vmatrix} 1 & 1 & 1 \\ V_1 & V_2 & V_3 \\ I_1 & I_2 & I_3 \end{vmatrix} = 0. \tag{A.1}$$

Subscripts 1, 2, and 3 denote the first, second, and third phasor measurements pairs, respectively. Considering

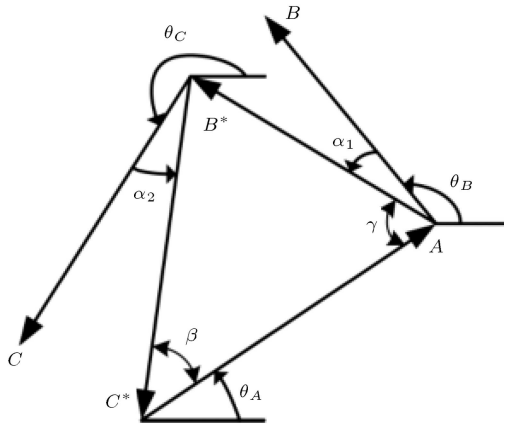

Figure A.1. Triangulation method to correct the phase drift.

the first measurement pair (V_1, I_1) as reference, then the phasor values whose undesirable phase drifts are corrected for the second and third measurements can be stated as $(V_2e^{-j\alpha 1}, I_2e^{-j\alpha 1})$ and $(V_3e^{-j\alpha 2}, I_3e^{-j\alpha 2})$, respectively. By substituting the corrected phasor values into Eq. (A.1), the following equation can be obtained:

$$A + B^* + C^* = 0, \tag{A.2}$$

where $B^* = Be^{j\alpha 1}, C^* = Ce^{j\alpha 2}$ and:

$$A = \begin{vmatrix} V_2 & V_3 \\ I_2 & I_3 \end{vmatrix}, \quad B = \begin{vmatrix} V_3 & V_1 \\ I_3 & I_1 \end{vmatrix}, \quad C = \begin{vmatrix} V_1 & V_2 \\ I_1 & I_2 \end{vmatrix}. \tag{A.3}$$

Eq. (A.3) states that if three measurements belong to a unique TE model, a triangular could be created from them, as shown in Figure A.1. Angles α_1 and α_2 could be either calculated from Eqs. (A.4) or (A.5) [19].

$$\begin{aligned} \alpha_1' &= \pi + \theta_A - \gamma - \theta_B, \\ \alpha_2' &= \pi + \theta_A + \beta - \theta_C, \end{aligned} \tag{A.4}$$

$$\begin{aligned} \alpha_1'' &= \pi + \theta_A + \gamma - \theta_B, \\ \alpha_2'' &= \pi + \theta_A - \beta - \theta_C. \end{aligned} \tag{A.5}$$

Biographies

Bahman Alinezhad Osbouei was Born in Mazandaran, Iran and received BSc degree in Electrical Engineering (Transmission and Distribution Systems) from Power and Water University of Technology (PWUT), Tehran, Iran in 2005. He received his MSc degree from the Department of Electrical Engineering from Sharif University of Technology, Tehran, Iran in 2007. He has been with Persian HV Substation Development Company for 7 years. Now, he is a Technical Engineer at Iran Grid Management Company (IGMC) and a PhD student at Shahid Beheshti University. His areas of interest include smart grid, power system protection, power system dynamic and simulation.

Hossein Kazemi Kargar received PhD degree from Amirkabir University, Tehran, Iran. Now, He is an Assistant Professor at Faculty of Electrical Engineering, Shahid Beheshti University, Tehran, Iran. His areas of research include power system protection, micro grids, smart grids, and power system optimization.